6-2007

Distributed Virtual Reality Simulation Assisted Steering Controller Design for Off Road Vehicle and Implement Tracking

Manoj Karkee
Iowa State University

Brian L. Steward
Iowa State University, bsteward@iastate.edu

Samsuzana Abd Aziz
Iowa State University

Distributed Virtual Reality Simulation Assisted Steering Controller Design for Off Road Vehicle and Implement Tracking

Abstract
For virtual reality simulation of off--road vehicles, real--time simulation must be achieved in spite of the heavy computational load from 3D graphics generation and numerical analysis of the dynamic model. In this work, a distributed architecture was developed for off--road vehicle and implement dynamic model and 3D graphics visualization to distribute the overall computational load of the system across two or more machines. This architecture consists of three major components: a dynamic model simulator, a virtual reality simulator for 3D graphics, and an interface to the controller hardware elements. Several off--road vehicle dynamics models have been developed with varying degrees of fidelity, as well as automatic guidance controller models and an interface to automatic guidance hardware. A towed implement model and an implement tracking steering controller developed. The performance of an implement position and heading feedback controller was similar to that of a tractor position and heading feedback controller. These models provide understanding into the behavior of automatically guided tractor--implement systems. In addition, the simulation and visualization system was effectively used to examine the practical limitations that the designed controller may face and to design the controller gains to adjust for those limitations.

Keywords
Real--time Simulation, Distributed Architecture, Virtual Reality, Vehicle Models, Implement Tracking, Steering Control

Disciplines
Bioresource and Agricultural Engineering

Comments
ASAE Paper No. 073006

American Society of
Agricultural and Biological Engineers

An ASABE Meeting Presentation
Paper Number: 073006

Distributed Virtual Reality Simulation Assisted Steering Controller Design for Off Road Vehicle and Implement Tracking

Manoj Karkee

Agricultural and Biosystems Engineering Dept., Iowa State University, karkee@iastate.edu.

Brian L. Steward

Agricultural and Biosystems Engineering Dept., Iowa State University, bsteward@iastate.edu.

Samsuzana Abd Aziz

Agricultural and Biosystems Engineering Dept., Iowa State University, suzana@iastate.edu

Written for presentation at the
2007 ASABE Annual International Meeting
Sponsored by ASABE
Minneapolis Convention Center
Minneapolis, Minnesota
17 - 20 June 2007

Abstract. *For virtual reality simulation of off-road vehicles, real-time simulation must be achieved in spite of the heavy computational load from 3D graphics generation and numerical analysis of the dynamic model. In this work, a distributed architecture was developed for off-road vehicle and implement dynamic model and 3D graphics visualization to distribute the overall computational load of the system across two or more machines. This architecture consists of three major components: a dynamic model simulator, a virtual reality simulator for 3D graphics, and an interface to the controller hardware elements. Several off-road vehicle dynamics models have been developed with varying degrees of fidelity, as well as automatic guidance controller models and an interface to automatic guidance hardware. A towed implement model and an implement tracking steering controller developed. The performance of an implement position and heading feedback controller was similar to that of a tractor position and heading feedback controller. These models provide understanding into the behavior of automatically guided tractor-implement systems. In addition, the simulation and visualization system was effectively used to examine the practical limitations that the designed controller may face and to design the controller gains to adjust for those limitations.*

Keywords. Real-time Simulation, Distributed Architecture, Virtual Reality, Vehicle Models, Implement Tracking, Steering Control

1. Introduction:

Tractors have played a vital role in the advancement of agricultural mechanization over the past several decades. One of the very common uses of tractors is to pull a towed implement. When it comes to auto-steering, most of the systems available in the market today are based on the control of the tractor position and heading. In many agricultural applications, however, accurately tracking a towed implement like a tillage implement or a towed sprayer may be equally or even more important than the accuracy needed for a tractor.

Studies have been carried out to model tractor-implement systems and to identify the problems associated with such systems. O'Connor (1997) demonstrated that a GPS-based automatic guidance system can be used to track rows in agricultural field with high precision. The control system was based on GPS measurements of position and heading of the tractor. This work, however, did not study the effect of implements on the dynamics and tracking accuracies. Bell (1997) developed dynamic models of a vehicle and a towed implement and created a vehicle and implement tracking controller. This work demonstrated that implement control is possible, but is more problematic due to the need of steering angles larger than the practical limit and difficulties in measuring position and attitude of the implement. Oksanen and Visala (2004) developed a 2D plane motion bicycle model of a tractor-trailer combination. The model was used to formulate optimal control problem of headland turning with tractor-trailer vehicle.

This research shows the potential of developing steering controllers for automatic guidance of an implement based on implement position and heading feedback as well as using the both implement and tractor feedback. However, such controllers must meet controller design criteria with system constraints such as maximum steering angle and rate. With the rise in model complexity, data quantity and computing power, we increasingly find ourselves lacking the tools and methods to deal with the information generated (Schulz et al., 1998). In the recent years, real time Virtual Reality (VR) simulation has been developed as a promising tool to deal with such complexities and challenges.

VR has been used in designing, modeling, and testing of vehicle designs and their control and also in studying the driver's perception and interaction with the new designs. For example, the National Advanced Driving Simulator (NADS) facility at the University of Iowa (Cremer et al., 1996) is an operator-in-the-loop simulation system which has been used in transportation studies, virtual prototyping and medical research. Schulz et al. (1998) developed a virtual environment for car-body engineering applications for visualizing virtual prototypes. The tool provided an effective way for engineers and managers to better communicate. Kang et al. (2004) developed a PC-based driving simulator as a testbed for simulating driving-related tasks. The system distributed model simulation and visualization tasks into two machines to share the computational load. Castillo-Effen et al. (2005) proposed a distributed architecture for modeling and visualization of multiple vehicles.

VR has also provided an environment for tele-operation and monitoring robots and autonomous vehicles. Lin and Kuo (1997) developed an underwater robot tele-operation system using VR. Gracanin el al. (1999) developed a VR testbed for mobile robots. The distributed system architecture consisted of a user interface, a data network and a navigation controller.

VR is also an effective tool for modeling off-road vehicle dynamics and designing vehicle controllers. However, when it comes to the simulation and visualization of dynamic models and control algorithms for off-road vehicles, the system has to deal with different complexities and to provide different functionalities as compared with the systems that are designed for on-road vehicles, under-water vehicles and airplanes. In most of the systems mentioned above, real-time simulation and visualization was not achieved, which is very critical in evaluating control algorithms. In addition, it is important that off-road vehicle simulation and visualization include

real terrain models in the virtual world, which are essential for studying vehicle dynamic behavior and safety scenarios in sloped terrain. Path planning for an autonomous agricultural vehicle must also take into account field operational performance. Thus, there is a need to develop simulation and visualization systems designed specifically for off-road agricultural machinery.

The objectives of this work were to:
- Develop a general-purpose, real-time, dynamic simulator for off-road vehicles in a virtual reality (VR) environment with controller-hardware-in-the-loop capability
- Develop a towed implement tracking steering controller and evaluate its performance using the simulation and visualization architecture.

2. The Simulation Architecture:

For virtual reality simulation of off-road vehicles, real-time simulation must be achieved in spite of the heavy computational load from 3D graphics generation and numerical simulation of the dynamics model. The primary goal of the work was to provide a real time simulation environment to the users, which is also flexible, extendable and scalable. To achieve this goal, a distributed Controller-Hardware-In-the-Loop (CHIL) vehicle simulation and visualization architecture (Fig. 1) was developed. In contrast to the classical concept of hardware-in-loop (HIL) system, which involves simulating a controller and putting a real machine in the loop, the CHIL system simulates the machine and put the hardware controller in the loop. This scheme will enable the simulation study of the performance of newly developed controller hardware and software. The scheme also enables the study of the vehicle dynamics models with the current controller hardware. The architecture consists of three components: a vehicle dynamics model, a VR geometric model and visualization system and a controller area network (CAN) interface to the hardware devices. The architecture provides the flexibility of distributing different components of the system across multiple processors to harness more computational capacity for the simulation. The interface was designed to incorporate navigation and steering controller hardware in the simulation loop.

In this architecture, the position and heading information produced by the vehicle model are sent to a GPS simulator which converts the position information into geographic co-ordinates (latitude, longitude and altitude). These data are next sent to the CAN interface software. Using this information, the CAN interface generates GPS messages and sends them to the navigation hardware. The navigation hardware scans and parses the GPS messages and generates guidance error messages. These errors are used by the steering controller hardware to develop a steering angle. The steering wheel angle is acquired and forwarded to the vehicle model. The vehicle dynamics model, on the other end, receives the steering angle and applies it as one of the inputs to the vehicle model completing the closed loop.

The VR simulation receives the position and heading information provided by the model and applies corresponding transformations to the geometric model to simulate the vehicle movement. The VR simulation is also responsible for estimating vehicle attitude based on the interaction of the vehicle model with the virtual world model and sending it back to the vehicle model.

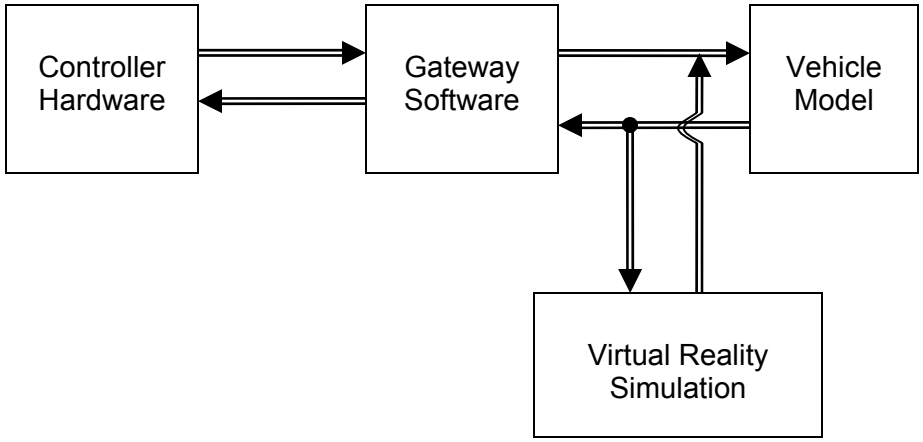

Fig. 1: Controller-Hardware-In-the-Loop (CHIL) simulation architecture. The block diagram shows the software and hardware components incorporated in the simulation system.

3. Implementation:

A prototype system was implemented based on the architecture described in the previous section. It was essential that the simulation and visualization system be flexible to allow modifications without major programming efforts (Castillo-Effen et al., 2005). Existing technologies were surveyed to identify the best candidates for an implementation that met the following three primary requirements.

1) Modifiable: Easy to modify the visualization environment as well as swap between available geometric and dynamic models
2) Portable across multiple environments
3) Extendable: Easy to extend the system to include more dynamic models and additional hardware interfaces

3.1 'Plug and Play' Modeling Environment and Dynamics Modeling:

MATLAB SIMULINK (The Mathworks, Natick, MA) was used as the modeling and simulation tool for the dynamic models. For simulations to be seamlessly integrated into the current and future VR applications, a data bus architecture was adopted for the models. This model structure enabled model component swappability for dynamic system models of vehicles and components.

A John Deere 8320 agricultural tractor was modeled with an autonomous guidance system. The system consisted of a vehicle model, a power train model, a navigation controller model or an interface to navigation controller hardware, a steering controller model or an interface to a hardware steering controller, a VR Interface and an internal data bus. In addition, a towed implement model and a steering controller to track the implement were developed. Each unit was modeled as a subsystem block with a self-contained set of inputs and outputs connected to the buses. Kinematic models of a tractor and a towed implement were developed. Higher fidelity dynamic bicycle and four wheel dynamic models were also developed for the tractor. These three models of the tractor offered varying model fidelities and computational demands.

3.2 VR Visualization:

The second component of the architecture is the VR visualization system. The VR system is based on a hierarchy of several programming tools including VR Juggler (VRJ, 2007), OpenSG (OpenSG, 2006) and OpenGL (OGL, 2007).

3.3 Controller Hardware Interface:

The third component of the simulation system was an interface to the controller hardware. Controller-Hardware-In-the-Loop (CHIL) auto-tracking simulation was implemented successfully to incorporate Deere & Co. navigation system and steering controller hardware. To run a CHIL simulation, hardware interface model blocks were inserted into the vehicle system model. As mentioned before, these blocks were swappable with the simulated controller model blocks. The CAN interface read in the messages from the model and sent them out over the CAN. Similarly, the interface read in the messages from the CAN and provided them to the vehicle model.

4. Development and Virtual Evaluation of Implement Tracking Steering Controller:

4.1 Kinematic Tractor and Implement Models:

Kinematic bicycle models were developed for a tractor and a towed implement (Fig. 2). A bicycle model assumes that the lateral forces in left and right wheels are equal. A kinematic model assumes that the vehicle moves in the direction that the tires are pointed, that is, there is no lateral tire slip in this model. The kinematic models represent the dominant dynamics of the tractor and the implement while keeping the models fairly simple and well understood. Additional dynamics will add higher order responses to the system and make it more complex. However, the dominant dynamics will not be altered much from the basic kinematic model. Because of these benefits, kinematic models are widely used as the first step in the research and simulation studies of the vehicle dynamics.

Common vehicle dynamics symbols were used to describe the dynamics of the tractor and the implement (Fig 2). The list of symbols is as follows.

- ψ heading angle of tractor
- V longitudinal velocity of tractor along vehicle center line
- δ_f steering angle
- L wheelbase of tractor
- y position of rear wheel of tractor in y- axis of the world co-ordinate system
- y_I position of wheel of implement in y- axis of the word co-ordinate system
- ψ_I heading angle of implement

- θ heading angle of implement relative to the tractor's longitudinal axis
- α angle between resultant velocity of hitch point and forward velocity
- V_{HLAT} lateral velocity of hitch point
- V_{ILON} longitudinal velocity of implement at pivot point along implement center line
- V_{ILAT} lateral velocity of implement at pivot point
- L_H distance of hitch point from rear tractor axle
- L_I distance from hitch point to implement axle.
- R turn radius of tractor
- R_I turn radius of implement

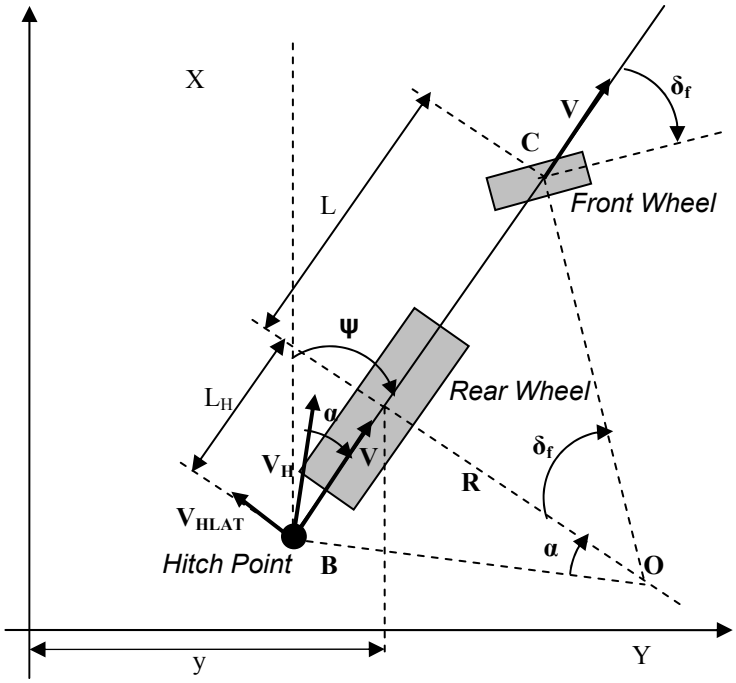

a)

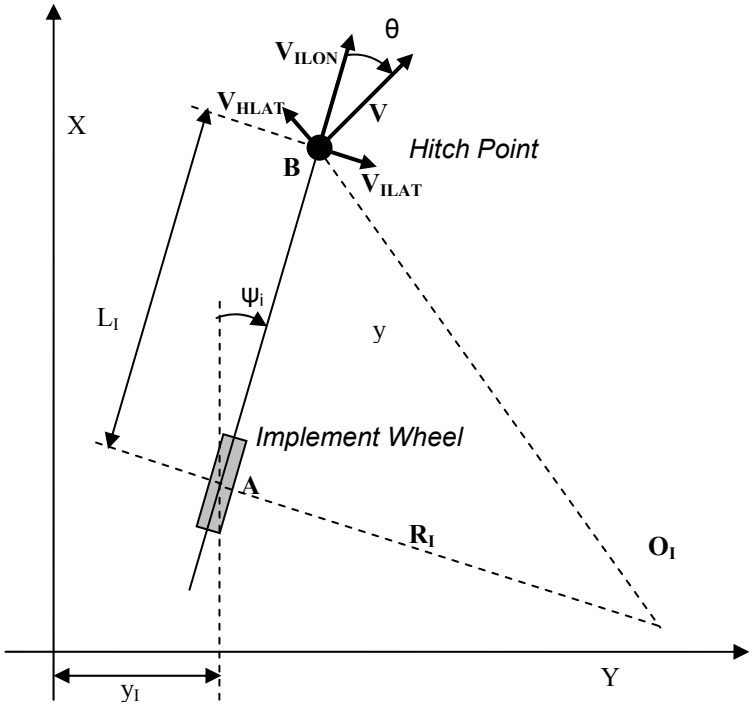

b)

Fig. 2: Kinematic bicycle model of a tractor (a) and a two wheeled towed implement (b). The implement parameters used in the model are of a typical grain cart.

The state equations for the kinematic tractor and implement model are:

$$\dot{y} = V \sin\psi \qquad (1) \qquad \dot{\psi} = \frac{V}{R} = \frac{V}{L}\tan\delta_f \qquad (2)$$

$$\dot{y}_I = \left(\frac{VL_H}{L}\tan\delta_f \sin\theta + V\cos\theta\right)\sin(\psi - \theta) \qquad (3)$$

$$\dot{\psi}_I = \frac{V}{L_I}\left[\sin(\psi - \psi_I) - \frac{L_H}{L}\tan\delta_f \cos(\psi - \psi_I)\right] \qquad (4)$$

The state equations were linearized and converted into transfer functions resulting in:

$$\frac{\Psi(s)}{\Delta(s)} = \frac{V}{Ls} \qquad (5) \qquad \frac{Y(s)}{\Delta(s)} = \frac{V^2}{Ls^2} \qquad (6)$$

$$\frac{\Psi_I(s)}{\Delta(s)} = \frac{\frac{VL_H}{L_I}\left(-s + \frac{V}{L_H}\right)}{Ls\left(s + \frac{V}{L_I}\right)} \qquad (7) \qquad \frac{Y_I(s)}{\Delta(s)} = \frac{\frac{V^2L_H}{L_I}\left(-s + \frac{V}{L_H}\right)}{Ls^2\left(s + \frac{V}{L_I}\right)} \qquad (8)$$

where: $\Psi(s)$, $\Delta(s)$, $Y(s)$, $\Psi_I(s)$, and $Y_I(s)$ are Laplace transformed variables corresponding to $\psi(t)$, $\delta_f(t)$, $y(t)$, $\psi_I(t)$, and $y_I(t)$, respectively.

Both tractor heading and position dynamics are neutrally stable. The open loop transfer function relating tractor heading to steering angle has one pole at the origin. The heading angle will thus have a ramp response for a step steering angle. Similarly, the open loop transfer function relating tractor position to steering angle has two poles at the origin, and will thus have a parabolic response to a step input. The implement heading and position dynamics (Eqns 7 and 8) are similarly related to each other. Both have an open loop pole at $-V/L_I$, which shows that the implement angle will exhibit a first-order response with a time constant of L_I/V and follow the path of the tractor when pulled forward by the tractor. In addition, both implement transfer functions have a zero in the right-half plane at V/L_H, which is due to the fact that the pivot point of the implement (or the hitch point) is located behind the tractor rear axle (Bell, 1997). Both implement transfer functions are non-minimum phase systems (Lumkes, 2002; Ogata, 1978).

4.2 Steering Controller based on the Tractor Position and Heading Feedback:

One of the objectives of this work was to design a steering controller to guide a tractor and a towed implement to a predefined track. Two different types of controllers were designed and analyzed to meet a number of design requirements. The first controller was based on the tractor position and heading feedback; the second controller was based on the implement position and heading feedback.

The tractor model is based on the parameters of John Deere 8320 tractor. Implement parameters chosen were from a typical two-wheel grain cart. Most of the analytical work is based on a forward velocity of 4.5 m/s (10 miles/hr). However, wherever possible and necessary, analysis was also carried out on a range of velocities to assess performance across that range. The tractor and implement parameters were L_H = 1.0 m, L_I = 5.5 m, and L= 2.97 m.

The design of the controller was guided by the following specifications:

1. The closed loop system must be stable.
2. The two percent settling time must be less than 16 s.
3. The maximum overshoot must be less than 10%,
4. The steady state error should be as small as possible.

Tractor Heading Control:

Since the tractor heading system is a first order neutrally stable system, a proportional (P) controller is adequate to stabilize the system (Fig. 3).

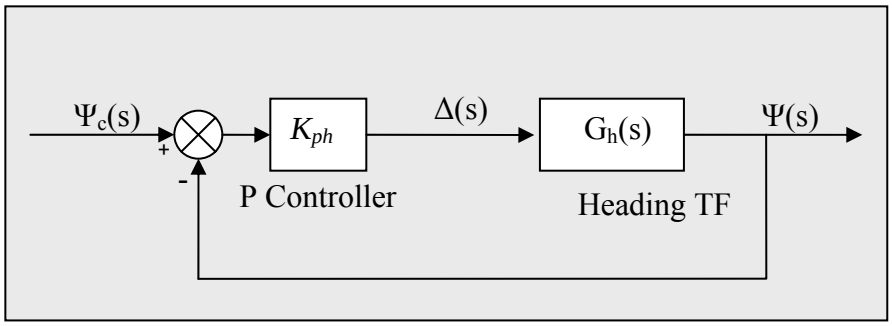

Fig. 3: Proportional control of the tractor heading system.

The closed loop transfer function is,

$$TF_{CL} = \frac{K_{ph}V}{Ls + K_{ph}V} \qquad (9)$$

where, the time constant, $\tau_{ph} = \frac{L}{K_{ph}V}$ (10)

The system is stable for any positive value of K_{ph}. Based on the design criteria of a settling time of 16 s, the time constant, τ_{ph} should be 4 s. Then using V = 4.5 m/s, the gain K_{ph} was 0.165 (from Eqn 10; Table 1, page 18). A proportional controller is sufficient to control tractor heading.

Tractor Position Control:

A proportional (P) controller is not enough to stabilize this system, since the open loop tractor position dynamics are second order neutrally stable. A derivative (D) controller added to the P controller will stabilize the system.

The position transfer function is $G_p(s)$ is given by Eqn 6. The controller transfer function is,

$$T_c(s) = K_{pp} + K_{dp}s \qquad (11)$$

The characteristics equation of the closed loop system can be used to find the individual gains that meet the design specifications. The closed loop transfer function of the system is

$$TF_{CL}(s) = \frac{K_{dp}V^2 s + K_{pp}V^2}{Ls^2 + K_{dp}V^2 s + K_{pp}V^2} \qquad (12)$$

where, time constant, $\tau = \frac{2L}{K_{dp}V^2}$ (13)

and, $$\zeta = \frac{VK_{dp}}{2\sqrt{K_{PP}L}} \qquad (14)$$

As before, setting the time constant of 4 s to achieve a 16 s settling time, and then solving for K_{dp} (Eqn13) results in: K_{dp} = 0.073. Setting the damping ratio to 0.707 will more than meet our maximum overshoot specification, and solving for K_{pp} (Eqn14) resulted in K_{pp} = 0.018.

The resulting gains were quite small, but reasonable, based on the rather large settling time specification. Before tightening the settling time specification, a PID controller was investigated to see if integral control might have any advantages in improving controller performance. For a PID controller, the controller transfer function is:

$$T_c(s) = \frac{K_{dp}s^2 + K_{pp}s + K_{ip}}{s} = \frac{K(s^2 + s + 1)}{s} \qquad (15)$$

where, $K = K_{dp} = K_{pp} = K_{ip}$. Then the open loop system transfer function is

$$TF_{OL}(s) = \frac{(K_{dp}s^2 + K_{pp}s + K_{ip})V^2}{Ls^3} = \frac{K(s^2 + s + 1)V^2}{Ls^3} \qquad (16)$$

The root locus of the system with equal controller gains (Fig. 4) reveals that the system is stable for a range of gains. However, a damping ratio larger than 0.5 can not be achieved by using equal P, I and D gains. Nevertheless, closed loop transfer function analysis and controller tuning provides more insights into the PID controlled system.

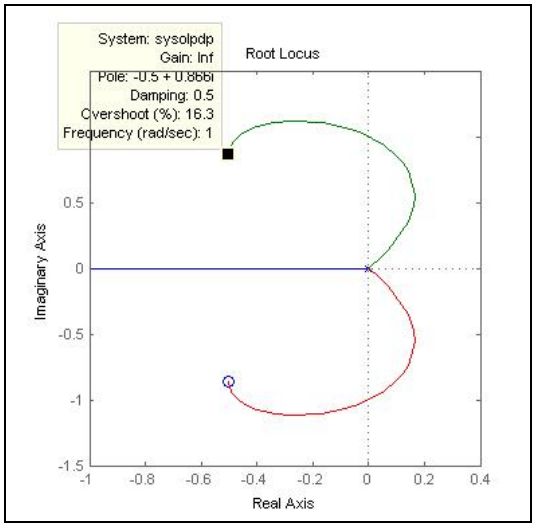

Fig. 4: Root locus of the tractor position with a PID controller assuming proportional, derivative and integral gains are equal.

The closed loop transfer function for the PID controlled system is,

$$TF_{CL}(s) = \frac{(V^2K_{dp}s^2 + V^2K_{pp}s + V^2K_{ip})}{Ls^3 + V^2K_{dp}s^2 + V^2K_{pp}s + V^2K_{ip}} \qquad (17)$$

Using the Routh-Hurwitz stability criteria (Palm, 2005), for L>0, K_{dp}, K_{pp}, and K_{ip} >0 and

$$V^4 K_{dp} K_{pp} > L V^2 K_{ip} \Rightarrow K_{ip} < \frac{V^2 K_{dp} K_{pp}}{L} \qquad (18)$$

for closed loop system stability.

Eqn 18 shows that for a small forward velocity V, which is typical in agricultural applications, K_{ip} has to be very small relative to K_{dp} and K_{pp} assuming they are both less than one. Based on the characteristic equation (denominator of Eqn 17), the dominant pole will be closer to the imaginary axis for the smaller K_{ip}. So, adding an integral controller has the effect of increasing system settling time. The use of an integral controller does not offer any improvements in overall controller performance as the steady state error to a step command input is already zero (Eqn 12). It may offer some advantages in driving steady-state disturbance error to zero, but since the integral gain must be so small, the integral effect will be slow in reducing steady-state error. Thus, in the end, a PD controller was used as the tractor position controller.

Revisiting the PD controller, controller gains were recalculated for a settling time of 7 s corresponding to a settling distance of 31.5 m at 4.5 m/s. The decreased settling time will increase the damped natural frequency, but as long as the system is highly damped, the overshoot will not be large. Based on a revised 7 s settling time and a damping rato of 0.707, the new gains were 0.09 and 0.165 for K_{pp} and K_{dp} respectively (Table 1, page 18).

Integrated Tractor Position and Heading Control:

Thus far, the heading and position controllers were designed independently of each other. However, the steering controller must control both tractor position and heading. The controllers designed in the previous sections were integrated (Fig. 5) and resulting dynamics were evaluated to see if they meet the design requirements.

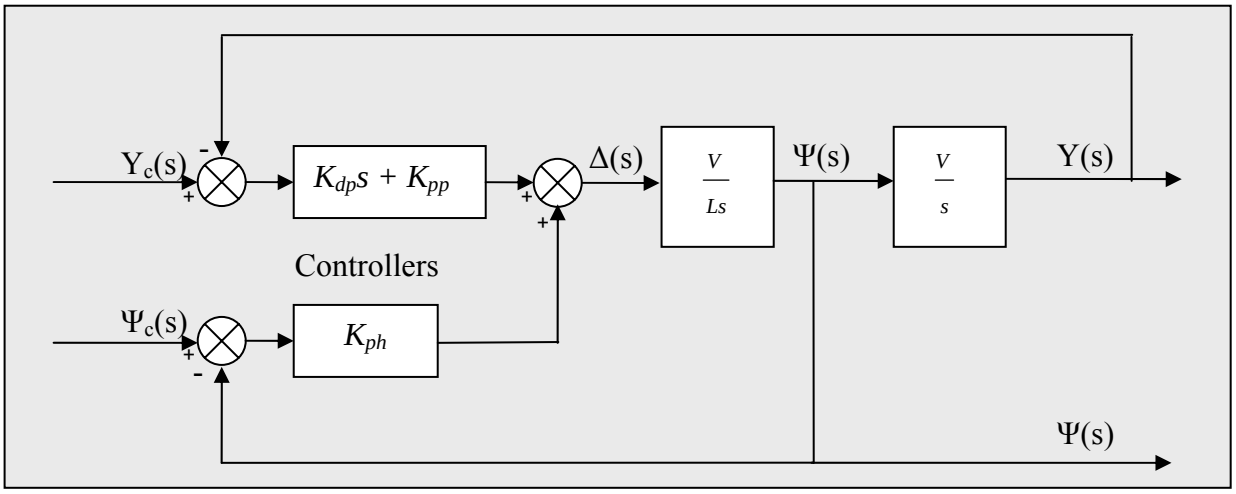

Fig. 5: Integration of the tractor position and heading controllers

The closed loop transfer function relating Y(s) and $Y_c(s)$ is,

$$TF_{CL}(s) = \frac{k_{dp} V^2 s + k_{pp} V^2}{L s^2 + \left(K_{ph} V + k_{dp} V^2\right) s + k_{pp} V^2} \qquad (19)$$

The system is still stable for positive gains, and the proportional heading term increases the system damping and decreases the settling time. Using the previously calculated values for the

gains, K_{dp} =0.165 ,K_{pp}= *0.09*, and K_{ph}=0.165, the damping ratio was 0.86 (maximum overshoot = 0.55%) and the settling time was 5.82 s.

Since the tractor is pulling the implement, we were interested in implement position response to tractor position command to compare with the implement position and heading feedback controller. The transfer function relating the implement position $Y_I(s)$ and the tractor position command $Y_c(s)$ was found to be:

$$TF_{CL} = \frac{V^2 \frac{L_H}{L_I}\left[-K_{dp}s^2 + \left(K_{dp} - K_{pp}\right)s + K_{pp}\frac{V}{L_H}\right]}{\left[Ls^2 + \left(K_{ph}V + k_{dp}V^2\right)s + k_{pp}V^2\right]\left(s + \frac{V}{L_I}\right)} \quad (20)$$

The characteristics equation of the implement position (denominator of Eqn 20) and tractor position (denominator of Eqn 21) were similar except an additional real pole in the implement position characteristics equation. This additional pole tended to make the system slower. The resulting response had a time constant of 1.98 s (settling time = 7.92 s). The implement heading dynamics were also same as the position dynamics. Maximum overshoot of the responses were less than 1%.

4.3 Steering Controller based on the Implement Position and Heading Feedback:

The integrated steering controller developed in the previous sub-section was based on the tractor position and heading feedback. As long as there are no disturbances, the position and heading of a towed implement can easily and accurately be calculated from the dynamics and static relationship between a tractor and an implement. However, in practice, several obstacles in the field may limit an implement to accurately maintain the ideal geometry and dynamics with the pulling tractor. For the successful application of auto-steering system in the field operations like tillage and spraying, a steering controller should be able to track the implement as accurately as possible. To increase the accuracy and reliability of implement tracking, there is a potential for feeding implement heading and position back to the steering controller. An integrated implement position and heading controller was thus developed using feedback from an implement mounted sensor.

Implement Heading Control:

Since the implement heading system has one pole at the origin, a P controller may be sufficient to control the system. The closed loop transfer function of the implement heading with a P controller is given by,

$$TF_{CL} = \frac{K_{ph}\frac{VL_H}{LL_I}\left(-s + \frac{V}{L_H}\right)}{s^2 + \left(\frac{V}{L_I} - K_{ph}\frac{VL_H}{LL_I}\right)s + K_{ph}\frac{V^2}{LL_I}} \quad (21)$$

The characteristics equation (denominator of Eqn 22) of the system shows that the system will be stable only if $K_{ph} < \frac{L}{L_H}$ (22)

We have, damping ratio, $\zeta = \dfrac{\left(\dfrac{V}{L_I} - K_{ph}\dfrac{VL_H}{LL_I}\right)}{2V\sqrt{\dfrac{K_{ph}}{LL_I}}}$ (23)

and, time constant $\tau = \dfrac{2}{\left(\dfrac{V}{L_I} - K_{ph}\dfrac{VL_H}{LL_I}\right)}$ (24)

Again, setting the damping ratio to 0.707 will more than meet our maximum overshoot specification, and solving for K_{ph} (Eqn 24) results in K_{ph} = 0.23. The controller gain satisfied the stability condition given by Eqn 23. The resulting settling time was 10.6 s (from Eqn 25, Table 1, page 18), which also met the settling time specification of 16 s. A proportional controller is sufficient to control implement heading.

Implement Position Control:

As mentioned before, a P controller is not adequate and an I controller does not provide much benefit if a plant is neutrally stable with more than one poles at the origin. Since the implement position is also a neutrally stable system with two poles at the origin, a PD controller could be a good choice for the implement position tracking. The unity feedback closed loop characteristic equation with a PD controller is,

$$Ls^3 + \left(\frac{LV}{L_I} - K_{dp}V^2\frac{L_H}{L_I}\right)s^2 + \left(K_{dp}\frac{V^3}{L_I} - K_{pp}\frac{V^2L_H}{L_I}\right)s + K_{pp}\frac{V^3}{L_I} = 0 \qquad (25)$$

From the Routh-Hurwitz stability criteria (Palm, 2005),

1. $\dfrac{LV}{L_I} > K_{dp}V^2\dfrac{L_H}{L_I} \Rightarrow K_{dp} < \dfrac{L}{VL_H}$ (26)
2. $K_{dp}\dfrac{V^3}{L_I} > K_{pp}\dfrac{V^2L_H}{L_I} \Rightarrow K_{pp} < \dfrac{V}{L_H}K_{dp}$ (27)
3. $\left(\dfrac{LV}{L_I} - K_{dp}V^2\dfrac{L_H}{L_I}\right)\left(K_{dp}\dfrac{V^3}{L_I} - K_{pp}\dfrac{V^2L_H}{L_I}\right) > LK_{pp}\dfrac{V^3}{L_I}$ (28)

So, the system is potentially stable for the selected ranges of K_{pp} and K_{dp}.

Finding the ranges of K_{pp} and K_{dp} under the constraint in Eqn 29 is algegraically complex. To simplify the controller gain tuning process, at first, just derivative control was used. Setting the damping ratio to 0.707, the resulting derivative gain K_{dp} was 0.05, which gave a settling time of 10.8 s. This derivative gain satisfied the constraint defined by Eqn 27.

The constraints defined by Eqns 28 & 29 and the K_{dp} value of 0.05 suggested that the controller gain K_{pp} must be smaller than 0.11 to make the system stable. Starting from this limiting value of 0.11, the gain K_{pp} was slowly decreased and the performance parameters were evaluated in each step. The selected value of the controller gain K_{pp} was 0.007, which gave a complex pole damping ratio of 0.707 and a settling time of 13.8 s. The system will be stable for the range of longitudinal velocities from 0.15 m/s to 59 m/s.

Integrated Implement Position and Heading Control:

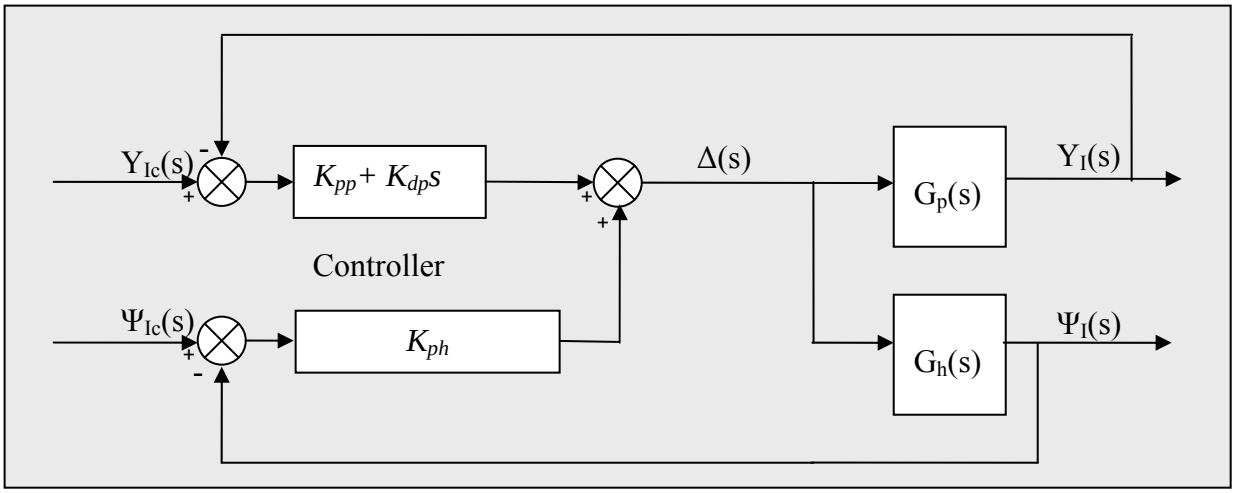

Fig. 6: Integration of implement position and heading controllers

The transfer functions $G_h(s)$ and $G_p(s)$ were given by Eqns 7 and 8 respectivelly. From the block diagram of the integrated controller (Fig. 6), the closed loop transfer function relating $Y_I(s)$ and $Y_{IC}(s)$ is found to be,

$$TF_{CL} = \frac{-K_{dp}V^2\frac{L_H}{L_I}s^2 + \frac{V^2}{L_I}\left(K_{dp}V - K_{pp}L_H\right)s + K_{pp}\frac{V^3}{L_I}}{Ls^3 + \frac{V}{L_I}\left(L - K_{ph}L_H - K_{dp}VL_H\right)s^2 + \frac{V^2}{L_I}\left(K_{ph} + K_{dp}V - K_{pp}L_H\right)s + K_{pp}\frac{V^3}{L_I}} \quad (29)$$

The characteristic equation (denominator of Eqn 32) shows that the system may be stable for different ranges of gains. From the independently designed controllers, the gains were 0.007, 0.05 and 0.23 respectively for K_{pp}, K_{dp}, K_{ph}. Using these gains and tractor and implement parameters, the closed loop transfer function becomes,

$$TF_{CL} = \frac{-0.18s^2 + 0.80s + 0.116}{2.97s^3 + 2.06s^2 + 1.65s + 0.116} \quad (30)$$

The roots of the closed loop characteristic equation of the system (denominator of Eqn 30) are:

s = -0.3084 ± 0.6427i (31) and s = -0.0769 (32)

The closed loop integrated implement heading and position control system was stable. However, the dominant settling time was about 52 s (Eqn 32). This performance parameter did not meet the design specification of 16 s.

The root locus plot (Fig. 7) of the open loop system was used in adjusting the controller gains for the better performance. This root locus was plotted by varying a gain *K*, which was equal to both the position proportional gain K_{pp} and the position derivative gain $K_{dp.}$ The heading proportional gain K_{ph} was fixed at 0.23. The new estimates of the controller gains K_{pp}, K_{dp} and K_{ph} were 0.01, 0.011 and 0.23 respectively. With these controller gains, the real parts of the poles were almost equal and thus none dominated the system response. The time constant was about 3.8 s (2% settling time 15.2 s). The damping ratio of the complex conjugate pole pair was 0.52 (Maximum Overshoot = 15%). This maximum overshoot was above the design specification of 10%. However, the first order pole in the characteristic equation tended to pull the total response down thus reducing the maximum overshoot. In fact, for the closed loop system, the maximum overshoot of the unit step response was less than 1% and the settling time was about 10.2 s (Fig. 8).

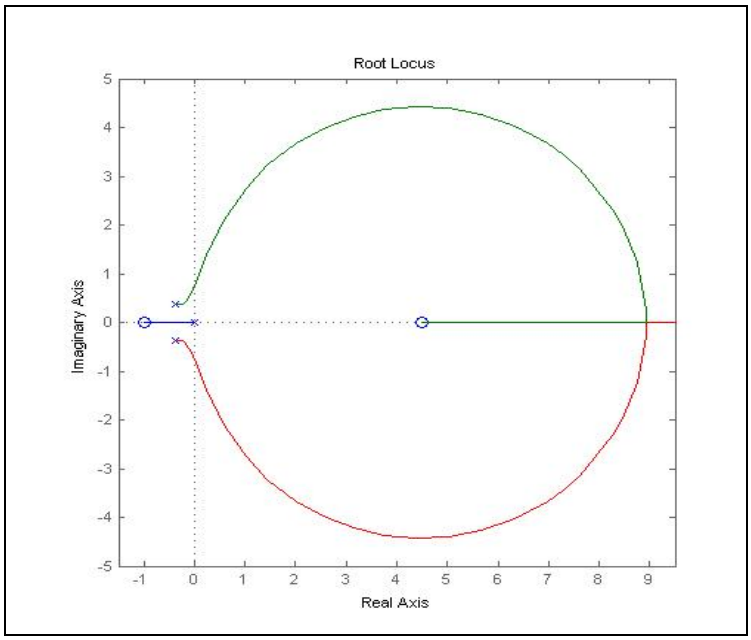

Fig. 7: Root locus of the integrated implement position and heading controller open loop system. The proportional and derivative gains of the controller were assumed to be equal.

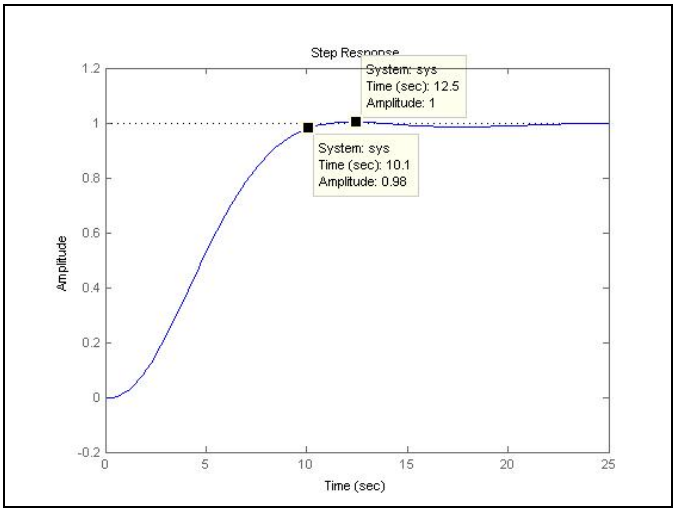

Fig. 8: Step response of the integrated implement position and heading controller closed loop system. The maximum overshoot is less than 1% and the two percent settling time is about 10 s. These performance parameters safely satisfy the design specifications.

The performance of the integrated controller depends on the operating longitudinal velocity. The controller was stable for a wide range of velocities from 0.1m/s to 60 m/s. The performance of the implement position and heading controller was within the design specifications for an operating velocity range from 1.5 m/s to 6.5 m/s. The settling distance specification was 72 m (4.5 m/s x 16 s). The settling distance of the system was within the limit of 72 m for a velocity range from 1.5 m/s to 6.5 m/s. The maximum overshoot was less than 10% for a velocity range from 0.5 m/s to 30 m/s.

The controllers designed in this work safely satisfied the design specifications set in the beginning of the design process (Table 1). For the longitudinal velocity of 4.5 m/s, the settling time of the integrated tractor position and heading controller (5.8 s for tractor dynamics and 7.9 s for implement dynamics) and the integrated implement position and heading controller (10.2 s

for implement dynamics) were well below the design settling time of 16 s. Similarly, both integrated controllers achieved a maximum overshoot of 4.0% or less, which was also well below the design specification of 10%.

Table 1: Controller gains, damping ratio, and settling time for different combinations of controllers and plants. Design specification for the two percent settling time and the maximum overshoot were 16 s and 10% respectively. The design longitudinal velocity was 4.5 m/s.

Plant		Controller Type	Gains			System Characteristics		
			K_{pp}	K_{dp}	K_{ph}	ξ	Max. Overshoot (%)	2% Settling Time (s)
Tractor	Heading	P Controller			0.17			16.0
	Position	PD Controller	0.090	0.17		0.71	4.0	7.0
	Integrated	P and PD controller	0.090	0.17	0.17	0.86	0.5	5.8/7.9*
Implement	Heading	P Controller			0.23	0.71	4.0	10.6
	Position	PD Controller	0.007	0.05		0.71	4.0	13.8
	Integrated	P and PD Controller	0.011	0.011	0.23		1.0	10.2

**The settling time of the tractor position and heading was 5.8 s and that of the implement position and heading was 7.9 s.*

Kinematic models of a tractor and implement system were developed with the full non-linear equations and added to the VR simulation and visualization environment described above. In addition, the two different steering controllers described above, based on linearized vehicle models were put into system. The simulation and visualization system was then used to simulate the non-linear tractor and implement models and the steering controllers. The performance of the controllers was evaluated using the simulation plots as well as VR visualization.

5. Simulation Results and Discussion:

The controllers responded to the initial heading and off-track error to bring them back to zero (Fig. 9). With the tractor position and heading controller, the settling time for the implement off-track error and the heading error was about 11 s (Fig 9 a). The analytical settling time for a step input was 7.9 s (Table1). Similar difference was observed with the tractor position and heading dynamics. The tractor position and heading settling times were 9 s and 5.8 s respectively from simulation and analytical result. The difference between simulated and analytical transient responses was perhaps due to the linearization applied to the analytical solution. The tractor and implement heading errors went up to 22° and 17° respectively after an initial tractor and implement heading error of 15° and tractor off-track error of 5m. The small angle assumption used in the linearization does not hold for such a big angle. Similarly, for the simulation with the implement position and heading feedback controller, the settling time was about 11.5 s for the off-track error and about 18 s for the heading error (Fig. 9 b). The analytical value of system settling time was 10.2 s. The difference is again because of the linearization applied to the state equations in analytical analysis. The performance of the implement position and heading controller was not much different than the performance of the tractor position and heading

controller. It shows that an implement tracking system could be developed using the feedback from an implement mounted position and heading sensor.

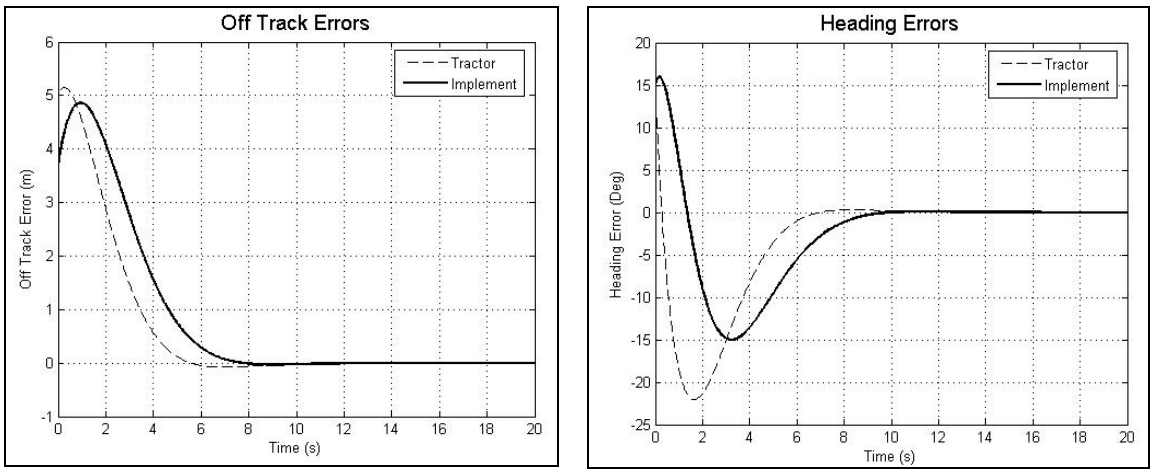

(a)

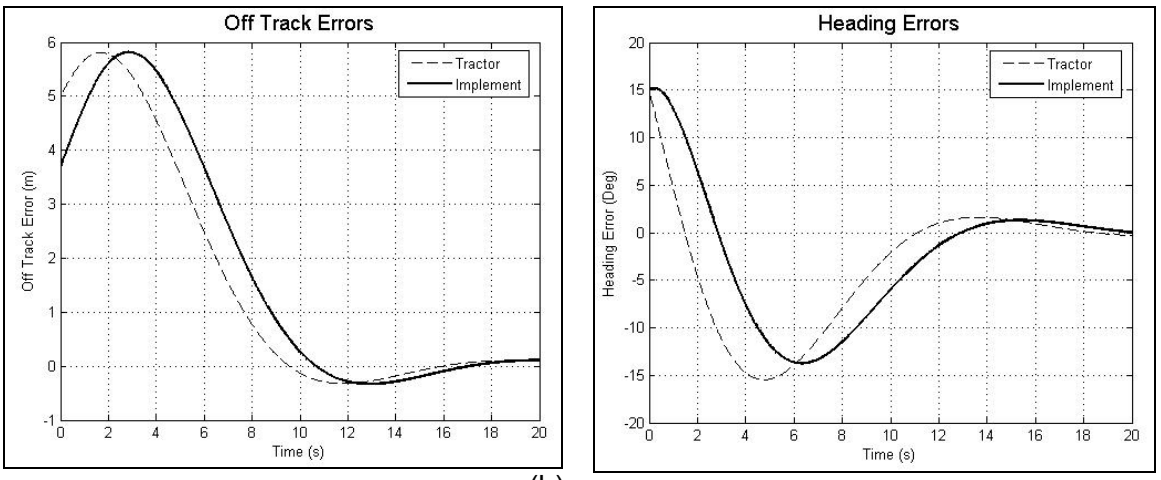

(b)

Fig. 9: Off-track and heading error of the implement with a) the tractor position and heading feedback controller, and b) the implement position and heading feedback controller.

Even though the analytical results and simulation curves look convincing, the steering controller may not meet the practical constraints of the tractor and towed implement tracking system such as maximum steering angle and rate. These practical limitations can easily be perceived in the VR visualization and the controller can be adjusted before going for a physical implementation and testing. Though it is not possible to completely avoid the need of physical testing, this process of VR rapid prototyping will significantly reduce the design and test cycle time. Through simulation and VR visualization, it was also observed the steering controller did not force the steering angle and steering rate to exceed their limits for initial off-track errors up to 7 m and initial heading errors up to 20°. The limiting steering angle and rate were assumed to be 30° and 6°/s respectively.

At BMW, engineers have observed that about 30% of the effort involved in a typical simulation goes into preprocessing and about 10% into actual computation. Approximately 60% goes into the analysis and communication of the results (Schulz et al., 1998). In this work, the VR visualization provided benefits in the analysis and the communication of the results. During the development of vehicle models and the implement tracking controllers, visualization played a

key role in reducing the effort on understanding the performance, post-processing of the simulation results, and effectively communicating them with the people involved.

6. Conclusions:

From this work, we can conclude that:

- A stable implement tracking system can be developed using the feedback from either the tractor mounted position and heading sensor or the feedback from implement mounted position and heading sensor.
- The controllers can satisfy the nominal design specifications of an off-road vehicle tracking system.
- A real-time simulation and VR visualization system could effectively be used in modeling off-road vehicles and designing and evaluating autonomous off-road vehicle controllers.

Acknowledgements:

This research was supported by Hatch Act and State of Iowa funds. (Journal paper of the Iowa Agriculture and Home Economics Experiment Station, Ames, Iowa, Project No. 3612.) The authors would like to thank Deere & Co. for their technical and financial support of this project.

References:

Bell, T. 1997. Precision Robotic Control of Agricultural Vehicles on Realistic Farm Trajectory. PhD dissertation, Stanford University.

Castillo-Effen, M., W. Alvis, C. Castillo, W. A. Moreno, and K. P. Valavanis. 2005. Modeling and visualization of Multiple Autonomous Heterogeneous Vehicles. IEEE International Conference on Systems, Man and Cybernetics. Oct 10-12, 2005. *The Hague, The Netherlands*.

Cremer, J., J. Kearney, and Y. Papelis. 1996. Driving Simulation: Challenges for VR Technology. *VR Blackboard column (ed. L. Rosenblum) in IEEE Computer Graphics and Applications*. 16-20, Sep1996.

Gracanin, D., M. Matijasevic, N. C. Tsourveloudis, and K. P. Valavanis. 1999. Virtual Reality Testbed for Mobile Robots. *IEEE International Symposium on Industrial Electronics*, Bled, Slovenia, July 12-16, 1999.

Kang, H. S., M. K. Abdul Jalil, and M. Mailah. 2004. A PC-based driving simulator Using Virtual Reality Technology. *Proceedings of ACM SIGGRAPH international conference on Virtual Reality continuum and its applications in industry*. Singapore, June 16-18, 2004.

Lin, Q., and C. Kuo. 1997. Virtual Tele-Operation of Underwater Robots. *Proceedings of the 1997 IEEE International Conference on Robotics and Automation*. Albuquerque, New Mexico, April 1997.

Lumkes, J. H. 2002. *Control Strategies for Dynamic Systems.* New York, N.Y., USA: Marcel Dekker, Inc.

O'Connor , M. L. 1997. Carrier-Phase Differential GPS for Automatic Control of Land Vehicles. PhD thesis, Stanford University, 1997.

Ogata, K. 1978. *System Dynamics*. Prentice Hall.

OGL. 2007. OpenGL, The Industry's Foundation for High Performance Graphics. Available at: www.opengl.org. Accessed 12 March 2007.

Oksanen , T. and A. Visala. 2004. Optimal Control of Tractor-trailer System in Headlands. *Automation Technology for Off-Road Equipment Conference.* Kyoto, Japan, 7-8 Oct, 2004.

OpenSG. 2006. OpenSG. Found at: www.opensg.org, accessed 14 February 2006.

OSG. 2007. OpenSceneGraph. Available at: www.openscenegraph.com. Accessed 12 March 2007.

Palm, W. J. 2005. *System Dynamics*. New York, N.Y., USA: The McGraw-Hill Companies, Inc.

Schulz, M., T. Reuding, and T. Ertl. 1998. Analyzing Engineering Simulations in a Virtual Environment. *IEEE Computer Graphics and Applications archive*, 18(6): 46 – 52.

Stombaugh, T. S., E. R. Benson, and J. W. Hummel. 1998. Automatic Guidance of Agricultural Vehicles at High Field Speeds. ASAE Meeting Presentation. Paper No. 983110.

Van Zuydam, R. P. 1998. Centimeter-Precision Guidance of Agricultural Implements in the Open Field by Means of real Time Kinematic (RTK) GPS. 4th International Conference on Precision Agriculture. Saint Paul, MN, 19-22 July, 1998.

VRJ. 2007. VR Juggler. Available at: www.vrjuggler.org. Accessed 12 March 2007.